Water Research 288 (2026) 124715

Contents lists available at ScienceDirect

Water Research

journal homepage: www.elsevier.com/locate/watres

Validating a Bayesian network model to characterise faecal indicator organism loss from septic tank systems in rural catchments

Chisha Chongo Mzyece [a,b,d,*], Miriam Glendell [b], Zisis Gagkas [b], Mads Troldborg [c], Camilla Negri [b], Eulyn Pagaling [b], Ian Jones [a], David M. Oliver [a]

[a] Biological and Environmental Sciences, Faculty of Natural Sciences, University of Stirling, Stirling, FK9 4LA, United Kingdom
[b] Environmental and Biochemical Sciences Department, James Hutton Institute, Aberdeen, AB15 8QH, United Kingdom
[c] Information and Computational Sciences Department, James Hutton Institute Dundee DD2 5DA, United Kingdom
[d] Water and Environment Research Center, National Institute for Scientific and Industrial Research, Plot 15302, Lusaka, Zambia

HIGHLIGHTS

- Bayesian Network (BN) model developed to assess faecal pollution from septic tanks.
- BN model performance evaluated using FIO load and microbial source tracking data.
- Landscape features impacting FIO pollution of water from septic tanks identified.
- National scale FIO pollution from septic tanks explored via upscaled predictions.

GRAPHICAL ABSTRACT

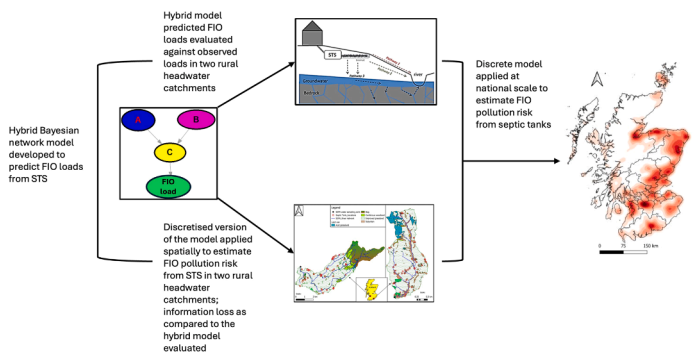

ARTICLE INFO

Key words:
Escherichia coli
Septic tanks
Bayesian networks
Water quality
Environmental pollution
Hydrological connectivity
Faecal bacteria

ABSTRACT

Validating model predictions with observed data is crucial for fostering confidence in model results, yet it is often overlooked in Bayesian Network (BN) studies. This research validated a BN model designed to predict faecal indicator organism (FIO) loss from septic tank systems (STS) in rural catchments. Both a hybrid model (combining continuous and discrete variables) and a fully discretised model were assessed in two test catchments. Our approach to model validation employed four methods: (1) comparing probability distributions of simulated and observed FIO loads in the hybrid model, (2) sensitivity analysis in the discrete model to identify key variables influencing results, (3) estimating percentage bias (PBIAS) to evaluate the average difference between predicted and observed FIO loads in the hybrid model, and (4) applying Shannon entropy to measure uncertainty in the spatial application of the discrete model. Predicted FIO loads per STS were consistent across models, with the hybrid network estimating 4.63×10^{10} cfu/yr in the Cessnock catchment and 4.36×10^{10} cfu/yr in the Mein catchment, while the discrete network predicted 3.85×10^{10} cfu/yr and 3.65×10^{10} cfu/yr, respectively, closely aligning with observed values of 6.17×10^{10} cfu/yr and 5.10×10^{10} cfu/yr. Sensitivity analysis identified STS condition and treatment level as critical factors influencing FIO loss. Shannon entropy values (1.60–1.85) revealed significant uncertainty in model predictions in the catchment where STS were

* Corresponding author.
E-mail address: c.c.mzyece@stir.ac.uk (C.C. Mzyece).

https://doi.org/10.1016/j.watres.2025.124715
Received 24 April 2025; Received in revised form 23 September 2025; Accepted 1 October 2025
Available online 2 October 2025
0043-1354/© 2025 The Author(s). Published by Elsevier Ltd. This is an open access article under the CC BY license (http://creativecommons.org/licenses/by/4.0/).

associated with a variability of Hydrology of Soil Types (HOST)-derived risk factors. When applied at national scale, greater confidence in model results was associated with Central, East and West Scotland where most STS were associated with a moderate to high HOST-derived risk classification. Our research is the first to show how BN models can predict FIO pollution from STS to watercourses and the findings suggest that refining model predictions requires more accurate data on STS treatment levels and maintenance, as well as access to good quality high-resolution water quality monitoring data.

1. Introduction

Septic tank systems (STS) are used worldwide for treating domestic wastewater in areas where conventional sewer networks are inaccessible, impractical, or costly, such as rural regions. For example, in the USA, approximately 18 % of households (equivalent to 21.7 million homes) utilise STS or cesspools (USEPA, 2021). Across Africa, there has been a notable increase in STS usage classed as improved sanitation which accounts for close to 40 % of sanitation development, particularly in peri-urban areas, to accommodate the expanding urban regions (African Development Bank, 2020). In Australia, 7 % of the population rely on onsite sewage treatment with ~93 % of the population being consistently linked to a public sewer network since 2010 (OECD, 2023). The prevalence of STS across Europe varies depending on factors such as urban population density and stringent local regulations regarding installation and maintenance. Conservative estimates suggest that ~4 % of the population in the UK rely on STS and small private sewage treatment systems for sewage disposal (Defra, 2002; O'keeffe et al., 2015; Richards et al., 2016).

Treating wastewater in STS primarily involves the settling of solids through primary sedimentation, which may be followed by additional treatment in soakaway fields. The effectiveness of this treatment relies on good STS maintenance, its age, and the filtration capacity of the surrounding soil (Beal et al., 2005). Poor maintenance, outdated infrastructure, and inadequate filtration of effluent can result in contaminated wastewater high in nutrient and faecal indicator organism (FIO) concentrations, which poses a contamination risk to both ground and surface water (Richards et al., 2016). While STS are recognised as potential sources of FIOs in rural catchments, there remain substantial knowledge gaps with respect to their overall contribution to water pollution (Mzyece et al., 2024). Although FIO removal rates of 50–95 % in conventional septic tanks have been documented (Kay et al., 2008), under certain environmental conditions, there is a possibility of bacterial proliferation, leading to higher FIO export from STS compared to the influent wastewater load (Appling et al., 2013). Microbial retention within soil pore architecture reduces FIOs available for transfer from land to water; however, further investigation is needed to fully understand the transfer dynamics of FIOs between soil compartments and groundwater (Bradford and Harvey, 2017), along with considering other environmental factors such as topography and proximity of STS to water bodies.

Mitigating FIO contamination is essential for preserving water quality and protecting public health, particularly in catchments that drain to recreational waters designated for bathing or to shellfish harvesting waters, both of which provide human exposure pathways to faecal pollution (Oliver et al., 2024). Water quality models play a vital role in helping to manage FIO pollution of water catchments; they can be used to predict pollution throughout the microbial source-mobilisation-delivery-impact continuum within landscapes (Glendell et al., 2022). For example, models can be applied at the catchment scale to predict *E. coli* burden on agricultural land from livestock sources, considering FIO accumulation and depletion over time (Oliver et al., 2018). Various hydrological models have been used to underpin predictions of nutrient and FIO pollutant transport, e.g., by estimating overland flow and utilizing pollutant export coefficient methods (Yuan et al. 2020). Additionally, multiple linear regression-based models use environmental factors to predict FIO loads at downstream receptors such as bathing beaches (Madani and Seth, 2020; Rossi et al., 2020).

Bayesian Networks represent another modelling approach for understanding FIO risks in the environment. Bayesian Networks (BNs) are probabilistic graphical models that represent a collection of random variables and their conditional dependencies through a Directed Acyclic Graph (DAG) (Pollino and Henderson, 2010). The structure of a BN illustrates causal relationships among components of a system. These models are composed of three fundamental elements: (1) nodes, which denote random variables within the system; (2) arcs, which indicate causal relationships between these variables; and (3) Conditional Probability Tables (CPTs), which quantify the strength of the relationships and are used to compute the probability distributions of the nodes. BNs utilise Bayes' theorem within a DAG framework—free from feedback loops—to model uncertainties and support decision-making processes, thus functioning as a form of Decision Support System (DSS) grounded in probability theory (Jensen, 1996; Pearl, 2014).

The application of BNs in environmental risk assessment of complex systems such as water catchments has been increasing (Phan et al., 2016). This is attributed to several of their characteristics, including good predictive power even when variables have missing data, which would result in imputation or omission in other models such as Markov chain, classification trees, and random forests (Moe et al., 2021). In our study, BNs were chosen for their flexibility in incorporating multiple data types, including expert judgements and for their ability to explicitly account for uncertainty. These attributes render them particularly suitable for modelling FIO pollution risk from STS, where monitoring data are sparse and the fate and transport of microbial contaminants are influenced by complex, interacting environmental processes. BNs inherently accommodate uncertainty analysis. This is achieved using CPTs to encode dependencies between variables, probability distributions to represent uncertainty in continuous parameters, and causal structures to describe environmental processes governing pollutant dynamics. Collectively, these features, underpinned by the stochastic nature of BNs, enable the quantification of both epistemic and aleatory uncertainties (Glendell et al., 2022; Sahlin et al., 2020) and facilitate the systematic identification of uncertainty sources within the model (Sperotto et al., 2019).

Despite their advantages, BN modelling applications face challenges, such as loss of accuracy from the discretisation of continuous variables (Kaikkonen et al., 2020; Rohmer, 2020; Fenton and Neil, 2018); difficulties in validating BNs developed solely from expert-elicited knowledge due to lack of observed data and limited quantification of model confidence demonstrated by credible intervals around posterior probability distributions (Marcot and Penman, 2019).

To overcome the challenges associated with BN modelling, our study employed a hybrid network that incorporates both discrete and continuous variables, following the methodologies of Glendell et al. (2022) and Aguilera et al. (2010) and a discrete network to assess the extent of information loss after discretisation. Additionally, we utilized monitoring data alongside expert-elicited data (Mzyece et al., 2024) to validate model outcomes against observed data. Model performance was assessed by comparing predictions with relatively high temporal resolution data from two rural catchments with similar grassland-dominated land use, no sewage treatment works (STWs) inputs and with available microbial source tracking (MST) data. This experimental design allowed us to semi-quantitatively evaluate the FIO model and distinguish

between FIO load from STS, STWs and livestock/wildlife. Model uncertainty was quantified by estimating the Shannon entropy index which sums the product of the probability of each model's outcome and the natural logarithm of that probability across all possible outcomes (Ellerman, 2021). This measure is appropriate for estimating uncertainty in random variables with discrete values (Feutrill and Roughan, 2021), making it suitable for the discrete version of our BN.

The overarching aim of our study was to develop and test a probabilistic BN model to better understand the contribution of STS to faecal pollution in rural catchments. Specifically, our study objectives were to: I) predict FIO load from STS in two rural test catchments in Scotland; II) evaluate BN model performance relative to observed FIO load, using MST to apportion human and ruminant contributions; and III) upscale the model to predict FIO pollution risk from STS at the national scale.

2. Methodology

2.1. Study catchments

Two study catchments in Scotland were used to predict annual FIO load. The Cessnock catchment (Latitude 55.54568, Longitude −4.39248; area 22 km^2) and Mein catchment (Latitude 55.06482, Longitude −3.22122, area 12 km^2) (Fig. 1), which are typical rural catchments that primarily rely on STS for domestic wastewater treatment, with no STWs or sewer overflows present (Scottish Water, 2025). For our study this helps to constrain uncertainty concerning the source of any human-derived FIOs within our observed data used to evaluate the model predictions, suggesting that all human-derived FIOs originate from STS. Importantly, historical FIO water quality monitoring data covering September 2018 to September 2019 is available for both catchments, which includes MST information that provides an indication of the relative contribution of livestock versus human FIO contributions necessary for validating our predictive model. Detailed descriptions of the catchment characteristics can be found in Glendell et al. (2022), while additional visual representations of primary land use, STS locations relative to the drainage network, and Scottish Environmental Protection Agency (SEPA) water monitoring sites are provided in Fig. 1.

The Cessnock and Mein catchments are situated in southwest Scotland, predominantly characterised by improved grassland (64 % and 65 % of land cover, respectively). The primary soil types are stagnosols (61 %) in Cessnock and cambisols (59 %) in Mein, both of which are classified as slowly permeable with a moderate to high risk of septic tank effluent movement (Gagkas et al., 2021; Hudson et al., 2012). In total there are 65 and 36 STS in the Cessnock and Mein catchments, respectively, inferred from modelled STS locations provided by the SEPA. Most STS (87 % in Mein and 90 % in Cessnock) are situated >50 m away from watercourses, with 13 % and 10 % respectively falling within the range of 10–50 m, and none closer than 10 m. Approximately 78 % of STS in Cessnock and 44 % in Mein are located on gentle slope gradients (0–5 %), while the remainder are situated on moderate slopes (>5–25 %). SEPA has established water quality monitoring points in Cessnock Water and Mein Water positioned at the outlet of each catchment. Parameters monitored at these outlets include water chemistry, discharge, FIOs (*E. coli* and intestinal enterococci), and MST targets.

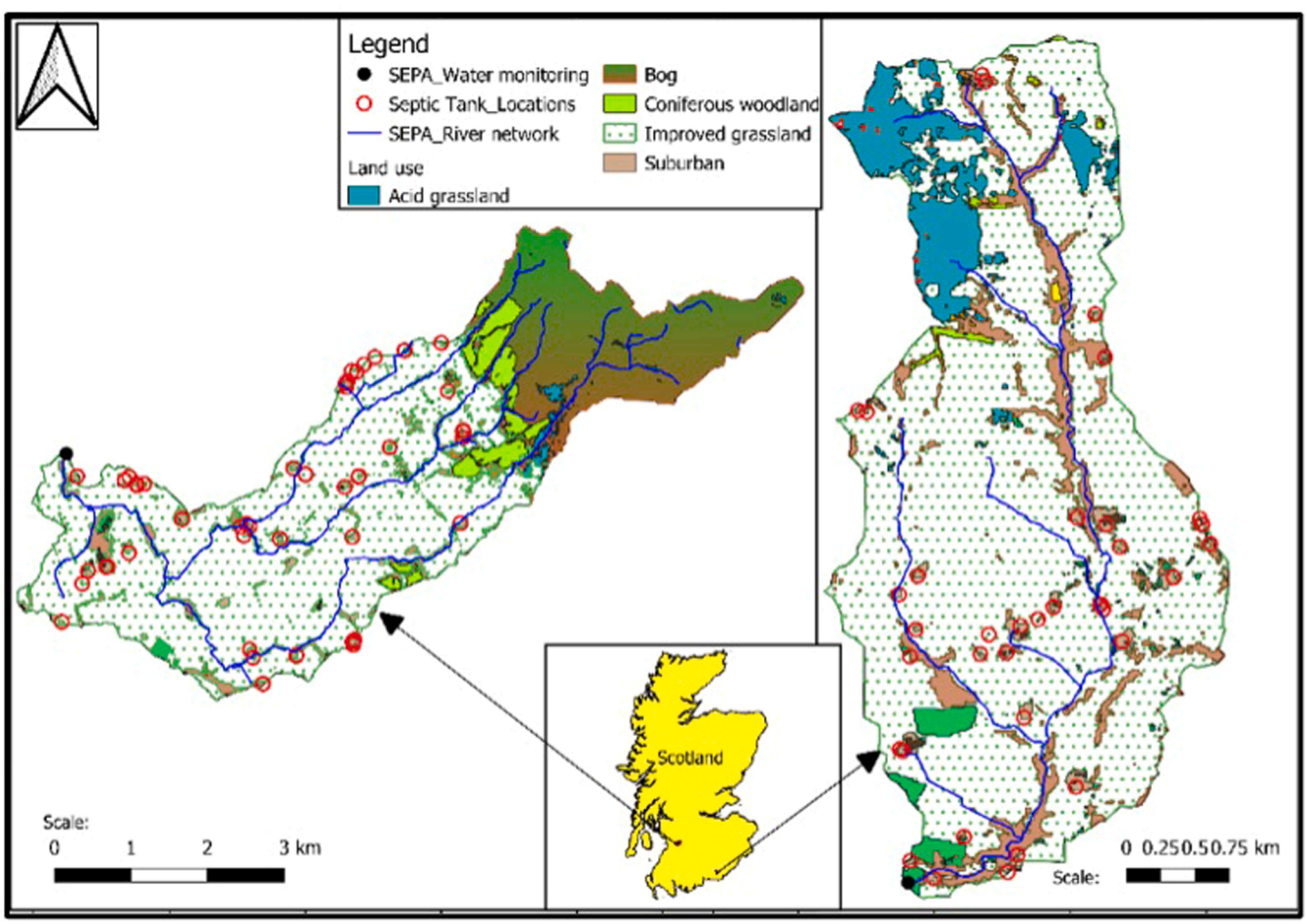

Fig. 1. Land use in the Cessnock and Mein catchments (Morton et al., 2024).

2.2. Model development and parametrisation

The model structure was modified from a phosphorus pollution risk model developed in Glendell et al. (2022). The detailed description of the nodes in the model along with their respective parametrisation methods is provided in the Supplementary Information, *SI 1*. Key datasets utilised for model parameterisation were STS locations from SEPA, FIO concentrations for different STS treatment levels obtained from literature (Gill et al., 2007; Kay et al., 2008), STS to watercourse FIO delivery proportions elicited from experts as detailed in Mzyece et al. (2024) and probabilities of effluent movement risk inferred from HOST-derived risk classifications (Gagkas et al., 2021). The model was developed in the proprietary Bayesian network software GeNIe vs. 4.1 (BayesFusion, 2024).

2.3. Model discretisation

To enable sensitivity analysis and spatial implementation, the model was discretised by converting continuous equation nodes into discrete chance nodes, as outlined in the GeNIe manual, Version 4.1 (BayesFusion, 2024). Two methods were employed to set discretisation boundaries: (i) equal intervals (dividing the continuous data into a predefined number of intervals with equal widths as seen in e.g., Aguilera et al. (2011) and Chen & Pollino (2012), and (ii) interpolation (a form of supervised discretisation (Beuzen et al., 2018) where boundaries were manually adjusted to obtain plausible probabilities). Initially, FIO load values in the target node (Realised FIO load) were logged to address skewness of the sample probability distribution (Nojavan et al., 2017). However, values in other equation nodes remained unlogged to allow FIO concentration calculations using original values. For equal intervals discretisation, the sample probability distribution specified by the lower and upper bound was divided into equal intervals representing the states in each of the equation nodes. Conditional Probability Tables (CPTs) were reviewed, and discretisation boundaries were adjusted through interpolation to obtain plausible probabilities for matching states (Low/Low, Medium/Medium, High/-High). This resulted in different marginal probabilities for the states in the Realised FIO load node between the two discretisation methods. To assess which method generated predicted FIO loads closer to the observed loads in the discrete network, we estimated the sum of squared errors (SSE). Based on the SSE and additional factors such as calculation of plausible probabilities in the CPTs and final marginal distributions in the target node, an appropriate discretisation method was selected.

2.4. Model evaluation

Model evaluation followed the approach of Glendell et al. (2022) and Troldborg et al. (2021), being implemented through four approaches: (1) sensitivity analysis to identify highly sensitive parameters that significantly affected reasoning in the model results; (2) comparing the distributions of predicted FIO load against observed FIO load in the two catchments; (3) calculating PBIAS to determine the difference between predicted and observed FIO load in the hybrid model; and (4) using Shannon entropy to assess uncertainty in the discrete version of the model applied spatially.

2.4.1. Sensitivity analysis

Sensitivity analysis was undertaken on the discretised version of the model to identify highly sensitive parameters that significantly affected reasoning in the model results. This was done within GeNIe 4.1, implementing the algorithm proposed by Kjaerulff & van der Gaag (2000). This algorithm calculated a set of derivatives of the posterior probability distributions over the target node (Realised FIO load) utilising each of the numerical parameters in the BN. Sensitive parameters were identified by observing the colour intensity of nodes in our BN and inspecting maximum node sensitivity values in the node properties table. Sensitivity analysis enabled targeted inspection of significant nodes to ensure correct parametrisation and therefore model outcomes.

2.4.2. Comparison of predicted against observed data

Two types of comparisons were made, namely the predicted versus observed catchment FIO load and the predicted versus observed FIO load per STS. Sections 2.4.2.1 and 2.4.2.2 describe the dataset including calculations made to enable comparison of observed values with model predictions.

2.4.2.1. Daily E. coli concentration. This dataset included 56 time-series data points for daily composite samples of *E. coli* concentration (cfu/100 ml) and daily mean discharge data (m^3/s) at the Cessnock outlet and 78 data points at the Mein outlet, between September 2018 and September 2019. Samples were collected twice weekly (Tuesdays and Thursdays) using 24-hour composite sampling with a refrigerated autosampler (Avalanche Teledyne ISCO). Each composite sample represents an integrated signal from 24 hourly subsamples, reducing the influence of short-term flow variability (Cassidy et al., 2018). Refrigeration has been shown to minimise FIO die-off during storage (Oliver et al., 2015).

Sampling was relatively consistent (~8 samples/month) between September–November 2018 and March–August 2019. However, coverage varied across sites and years: Cessnock had only 11 data points in 2019 compared to 51 at Mein, and both catchments had limited data (1–3 records) in December–January. No Cessnock samples were collected in June–July 2019. The full dataset is available on request and discharge–*E. coli* concentration plots are provided in the *SI 2* and *SI 3*. These plots demonstrate that FIOs were sampled across a broad range of discharge quantiles and indicate the minimum and maximum quantiles recorded in each catchment.

E. coli was selected as the most specific indicator of human-sourced faecal pollution (Price and Wildeboer, 2017) and therefore used in the validation. As our model aimed to estimate annual FIO load, we standardised the monitoring data to match the units in our model. First, the daily FIO load was calculated (Eq. (1)).

$$\textit{Daily FIO load} = EC_{1L} \times Q \tag{1}$$

where:

EC_{1L} *is the E. coli in 1* L, *and*

*Q is the Daily mean discharge (Q in L/second * 86,400* s*/day)*

Next, gaps in the data were filled by interpolation using two methods to ensure robustness. Last observation carried forward (LOCF) was undertaken in Excel by replacing missing data points with the last observed FIO load (Lachin, 2016). Additionally, linear interpolation was done in Python version 3.8 (Van Rossum and Drake, 2009) estimating missing values for FIO loads using linear regression. Daily mean FIO loads were then calculated separately for both methods, exported to GeNIe 4.1, and multiplied by 365 to obtain annual FIO loads. For each method, a distribution of 10,000 Monte Carlo simulations was generated and compared with the BN-predicted FIO load distribution. Potential uncertainties associated with interpolation are discussed in Section 4.

2.4.2.2. Using MST data. Microbial source tracking (MST) was performed using a multiplex qPCR assay targeting human- and ruminant-specific Bacteroides. Human-specific primers (HF183F/HF183R) and probe (BacHum193p) were applied as described by Seurinck et al. (2005) and Kildare et al. (2007), while ruminant-specific primers (BacR-F/BacR-R) and probe (BacR-P) followed Reischer et al. (2006). An internal amplification control (IAC) was included to detect inhibition. DNA was extracted from water samples using the DNeasy PowerWater Kit (Qiagen). qPCR reactions were prepared with BioRad iQ Multiplex Powermix, primers and probes for each target and the IAC, and up to 10 ng of template DNA, and run on a Bio-Rad CFX96. Standard curves were generated from plasmids containing target gene inserts, and only assays with efficiencies between 90 and 110 % were accepted. Absolute

abundances of human- and ruminant-specific Bacteroides were used for further analysis. MST sampling was conducted twice weekly for two years.

Since the observed annual total FIO load ($FIOload_{(OAT)}$) calculated from the *E. coli* concentration in Section 2.4.2.1 was indicative of *E. coli* from both human and animal sources, we used MST data available in both catchments to estimate the proportion of human-derived *E. coli* (*pHDE*) (Eq. (2)). Overall, average human Bacteroides concentrations were higher than ruminant Bacteroides over one-year sampling period in both catchments: 8.21×10^7 HuBac/L versus 6.89×10^5 RuBac/L in Cessnock, and 1.35×10^7 HuBac/L versus 7.18×10^5 RuBac/L in Mein. (See plots in *SI 4* and *SI 5*). The annual average proportion was then applied as a fixed factor to the $FIOload_{(OAT)}$ to derive the observed FIO load from human sources ($FIOload_{(HS)}$) (Eq. (3)). Next, the distribution of the $FIOload_{(HS)}$ per catchment was compared to that of the predicted FIO load per catchment in GeNIe and visualised using the ggdist R package (Kay, 2024).

$$pHDE = \frac{Hubac}{Hubac + Rubac} \tag{2}$$

where:

pHDE is the proportion of human-derived E. coli
Hubac represents human Bacteroides in 1 L*, and*
Rubac is ruminant Bacteroides in 1L

$$FIOload_{(HS)} = FIOload_{(OAT)} * pHDE \tag{3}$$

where:

$FIOload_{(HS)}$ *represents the FIO load from human sources per catchment*
$FIOload_{(OAT)}$ *is the observed annual total E. coli from both human and animal sources*
pHDE is the proportion of human-derived E. coli calculated in Eq. (2)

2.4.3. Estimation of model bias

Finally, we adopted the approach of Glendell et al. (2022) in using PBIAS to assess the model performance by comparing the model-predicted FIO load to the observed FIO load:

$$PBIAS = \left(\frac{\sum (X_{sim} - X_{obs})}{\sum X_{obs}}\right) \times 100 \tag{4}$$

where:

X_{sim} are FIO loads from 10,000 Monte Carlo model simulations at the catchment outlet and

X_{obs} are 10, 000 samples resampled from a truncated normal distribution fitted to observed *E. coli* data at the catchment outlet.

The distribution of the calculated bias was then observed, with closeness to zero indicating that the model predictions closely matched the observed data. Additionally, the bias distribution was discretised to establish an optimal interval ranging from −50 % to +50 %. Instances where probabilities fell below 50 % indicated that the model underestimated, whereas those exceeding 50 % indicated that the model overestimated.

2.4.4. Shannon entropy

The Shannon entropy index was used to evaluate uncertainty in the model outcomes in the spatial application of the discrete BN. Entropy was calculated over the target node in R by first defining the Shannon entropy function and then applying this function to each row representing a STS in our dataframe. Before performing the calculation, we verified that each row was numeric and removed any rows with a value of 0 to avoid log (0) errors. Shannon entropy was then calculated as follows:

$$H(X) = -\sum_{i=1}^{n} p_i \ln(p_i) \tag{5}$$

where:

- $p_i$is the probability associated with the state *i* of the target node
- *ln* (p_i) is the natural logarithm of the probability *pi*
- negative sign in front indicates that the sum is negated, ensuring that the entropy is a positive value.

The entropy quantifies the information content within a node; it equals zero if p_i is known with certainty and is maximised when p_i is unknown (Troldborg et al., 2021).

2.5. Spatial implementation of the discrete model

To predict annual FIO load per STS, we applied the discrete version of our BN spatially, firstly to the STS locations in our study catchments, and secondly to a national scale STS dataset in Scotland. The spatial application was done in R using the gRain (Hojsgaard, 2012) and bnlearn (Scutari, 2010) packages and basically involved using the BN model to simulate FIO load from each STS one at a time.

Spatial data, including X and Y coordinates of STS locations, distance to the nearest watercourse, slope inclination, and associated HOST_-derived risk factors, was loaded into R and discretised to match the BN states. The BN was then run with the spatial data for each STS, setting distance, HOST-derived risk, and slope as evidence, and the RealisedSTload as the target node. The resulting simulated probabilities were combined with spatial coordinates in a data frame and used to calculate the FIO load per STS.

2.5.1. Calculation and visualisation of FIO load per STS

The annual FIO load per STS was calculated as a sum of the mid values of the target node states weighted by their probabilities (*p*):

$$FIO\ load = p_1 * mid_1 + p_2 * mid_2 + \ldots + p_n * mid_n \tag{6}$$

where mid_n is the mid value of the nth state of the target node.

Maps were created in QGIS software version 3.82.2 (QGIS Development Team, 2021), to visualise FIO load for each STS in the study catchments and then upscaled to model FIO pollution risk from STS for the whole of Scotland. Further, STS points were weighted based on FIO load levels to differentiate risk categories: 1) STS with FIO load less than Quartile 1 assigned weight 1 and all other STS assigned 0; 2) STS with FIO load less than the median assigned weight 1, others 0; 3) STS with FIO load > Median assigned weight 1, others 0; and 4) STS with FIO load > Quartile 3 assigned weight 1, others 0. Maps were made for each category to help visualise pollution risk. A 5 mm heatmap radius was chosen to clearly show variations in pollution density.

3. Results

3.1. Model parameterisation

Fig. 2 presents the parameterised hybrid BN model, illustrating the posterior probability distributions for each variable. For continuous equation nodes and discrete nodes, distributions are visualized as histogram plots of samples and marginal likelihood proportions for different states, respectively. The nodes in the top left corner of the model visualisation pertain to variables related to STS site conditions within the catchments (in this case for Cessnock). The nodes in the top right corner of the model represent variables ('Distance', 'Slope' and 'Hydrology of Soil Types') associated with the connectivity between STS and watercourses, which influence the risk of STS effluent movement. The nodes in the middle section of the model calculate variables representing the FIO concentration (cfu/100 mL) based on STS conditions, followed by the resulting annual FIO load per STS. The target node, 'Realised FIO load', highlighted in red is our variable of interest calculating the FIO load per STS reaching a watercourse. In Fig. 2, this has

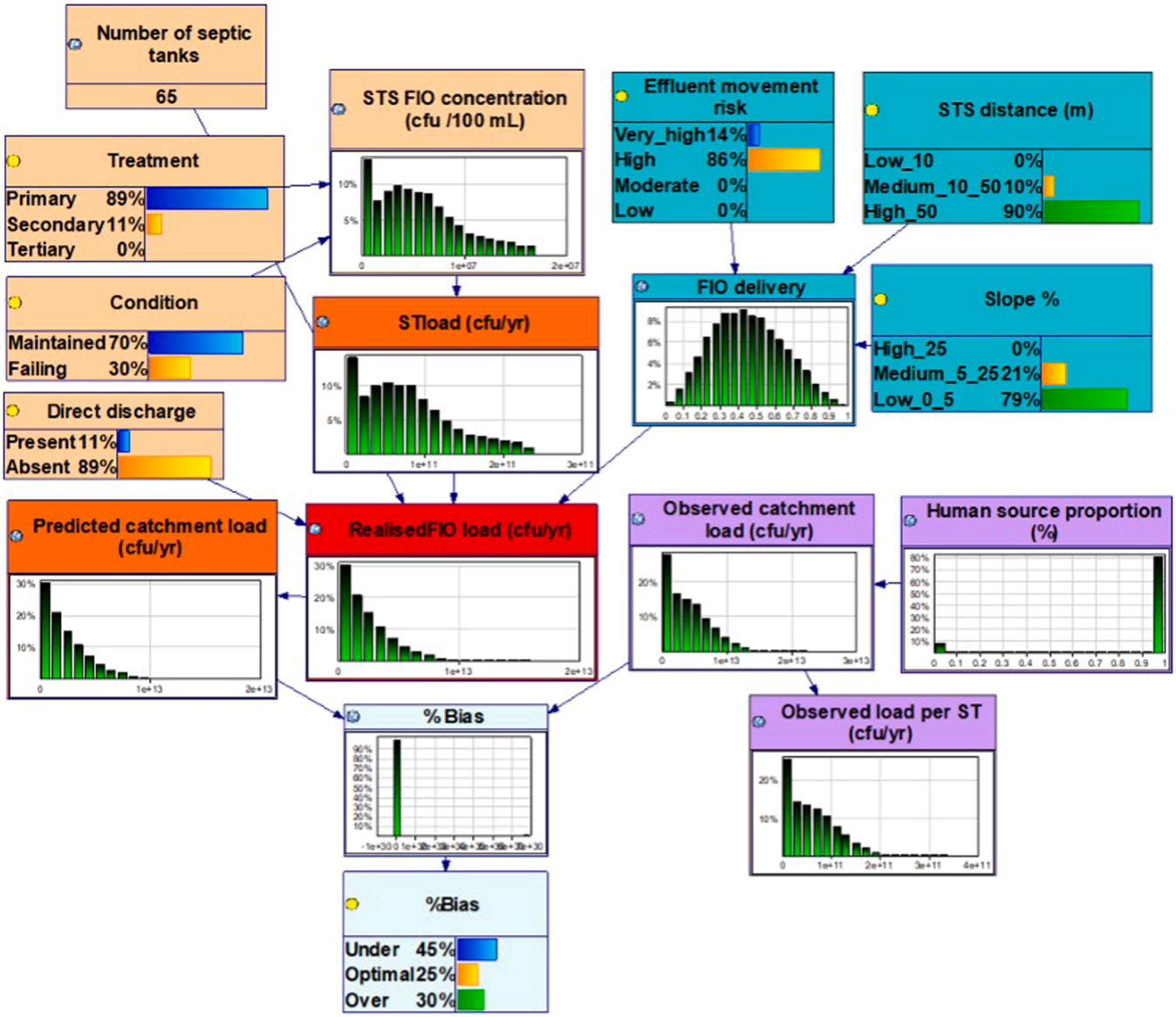

Fig. 2. Parameterised hybrid model showing 25 % optimal predictions, 45 % under optimum and 30 % over for the Cessnock catchment. Discrete nodes visualise probability distributions in form of bars of percentage likelihood of the states of the variable and equation nodes show this in form of a continuous histogram plot.

been multiplied by the number of STS in Cessnock to give the annual total catchment FIO load from STS. The 'Predicted load' node is a dummy node, equivalent to the 'Realised FIO load' node, added for convenient calculation of bias relative to the observed load. Bias is visualized as a continuous distribution of values around zero in an equation node and as a discrete node showing the overall model performance compared to observed data where ± 50 % bias is considered acceptable.

3.2. Model discretisation

Equal intervals were chosen as a more accurate discretisation method for the BN model's sensitivity analysis and spatial application. This choice was based on the following factors: no instances of over/under estimating probabilities in the CPTs, lower SSE and standard deviation (SD) (see Table 1), and lower Shannon entropy values compared to interpolation.

Unlike interpolation, which occasionally overestimated probabilities in the CPTs, for scenarios where lower probabilities were expected and vice versa, (e.g., 91 % for Realised FIO load without direct discharge vs. 62 % with direct discharge), there were no instances of such calculation errors observed after equal intervals discretisation. Although there were some differences in state boundaries (as shown in Table 1) and marginal probabilities, both methods produced similar results. Calculated marginal probabilities from equal intervals for the five states in the target node (Realised FIO load) are shown in Fig. 3. Recalculated marginal probabilities after interpolation were 5 % Very low, 6 % Low, 51 % Medium, 36 % High and 2 % Very high.

3.3. Model evaluation

3.3.1. Sensitivity analysis

Sensitivity analysis revealed that the primary factors affecting FIO pollution risk from STS were the treatment level and condition of the tank. These influenced the FIO concentration and subsequently the FIO load from the STS. Effluent directly discharged from STS to watercourses greatly affected the realised FIO load to a watercourse. The proportion of FIO delivery was primarily influenced by the HOST-derived risk, and to a lesser extent, by distance and slope. Fig. 3 illustrates the importance of these factors, with red shading indicating their significance and

Table 1
Comparison of predicted $\log_{10}$ annual FIO load per STS from equal intervals discretisation and interpolation.

	State/Statistic	Unit	Method		
			Equal intervals	Interpolation	Observed
States boundaries	Very low		4 - 6.2	4 - 8.9	
	Low		6.2 - 8.4	8.9 - 9.5	
	Medium		8.4 - 10.6	9.5 - 10.8	
	High		10.6 - 12.8	10.8 - 12.8	
	Very high		12.8 - 15	12.8 - 15	
Cessnock	Mean	($\log_{10}$cfu/yr)	10.54	10.55	10.79
	SD		1.44	1.48	–
	SSE		59,936	60,401	–
Mein	Mean	($\log_{10}$cfu/yr)	10.49	10.51	10.71
	SD		1.43	1.74	–
	SSE		57,988	67,519	–

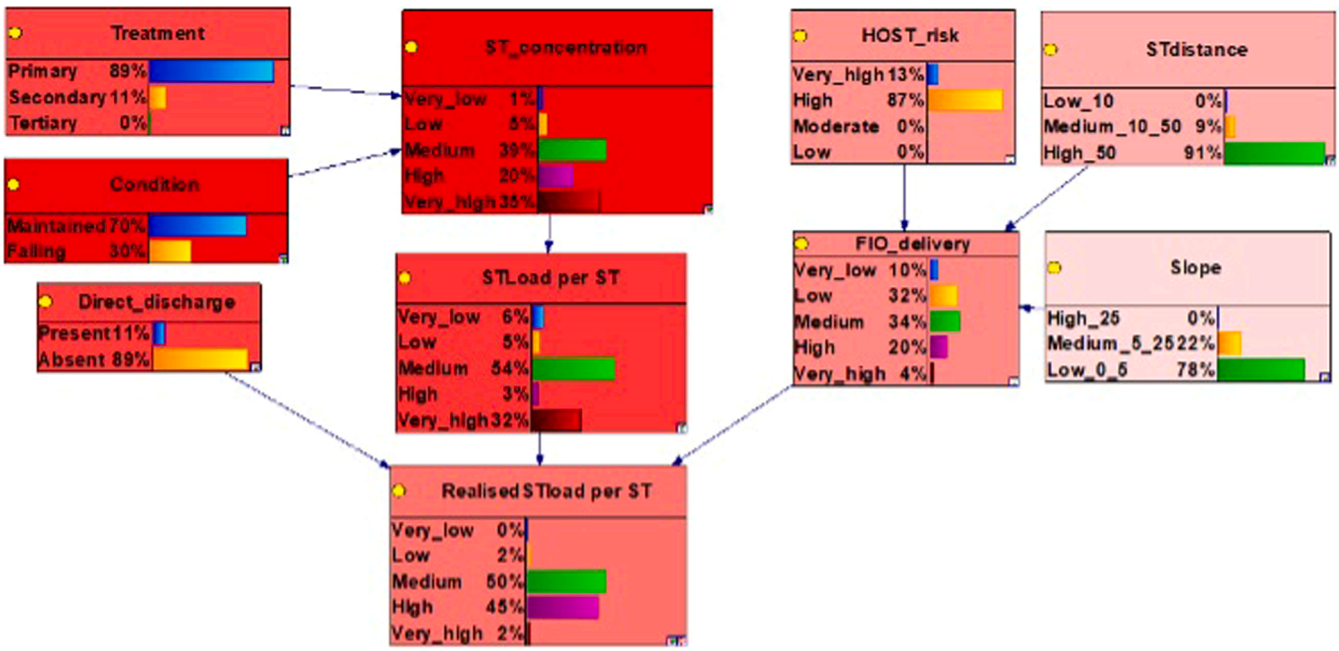

Fig. 3. Results of model discretisation showing marginal probability distributions for states in all the model variables and sensitivity analysis showing most influential factors in deep red shading in the Cessnock catchment.

summary information relating to the sensitivity of each node is provided in Table 3.

3.3.2. Validation against observed data

Overall, model predicted loads were comparable to the observed FIO loads, as illustrated in Fig. 4 and statistical summary given in Table 2. Both predicted and observed loads were of the same order of magnitude, although the predicted loads were lower than the observed loads. This underprediction is confirmed by negative PBIAS values in the hybrid model and observed in the discrete model. In Cessnock, the discrete model under predicted 52 % of FIO load values which fell below the acceptable bias threshold of 50 %, while 22 % were within the acceptable range of ±50 %, and 26 % were overpredicted, when compared to observed values from LOCF interpolation. When compared against linearly interpolated observations, simulation bias showed slight improvement, with 45 % underprediction, 25 % within the acceptable range, and 30 % overprediction. In the Mein catchment, the model showed significant underprediction at 83 %, with only 5 % falling within the acceptable range and 33 % being overpredicted when compared to observed values from linear interpolation. However, against observations from LOCF interpolation, model performance improved, with underprediction at 42 %, 25 % within the acceptable range, and 33 % overprediction.

3.4. Spatial implementation of the model

The predicted FIO load per STS was generally higher and showed less variation in the Cessnock catchment (ranging from 3.51×10^{10} to 4.81×10^{10} cfu/year) compared to Mein (1.22×10^{10} to 4.51×10^{10} cfu/year) (Fig. 5).

In Cessnock, STS with the lowest FIO load (3.51×10^{10} cfu/year) were linked to a high HOST-derived risk factor, positioned at least 50 m from a watercourse on a gentle slope (0–5 %). When the slope increased to 5–25 %, FIO load increased to 4.04×10^{10} cfu/year, indicating a 13 % increase due to slope variation. In contrast, STS located closer (10–50 m from a watercourse) produced an FIO load of 4.57×10^{10} cfu/year, reflecting a 23 % increase due to reduced distance. The highest FIO load in Cessnock (4.81×10^{10} cfu/year) was observed in STS with a very high HOST-derived risk factor, situated at least 50 m from a watercourse on a moderate slope (5–25 %).

In Mein, only 8 % of STS (three units) showed the lowest FIO load (1.22×10^{10} cfu/year). These were characterized by a low HOST-derived risk factor, a distance of at least 50 m from a watercourse, and a slope of 5–25 %. The highest FIO load in Mein (4.51×10^{10} cfu/year) was linked

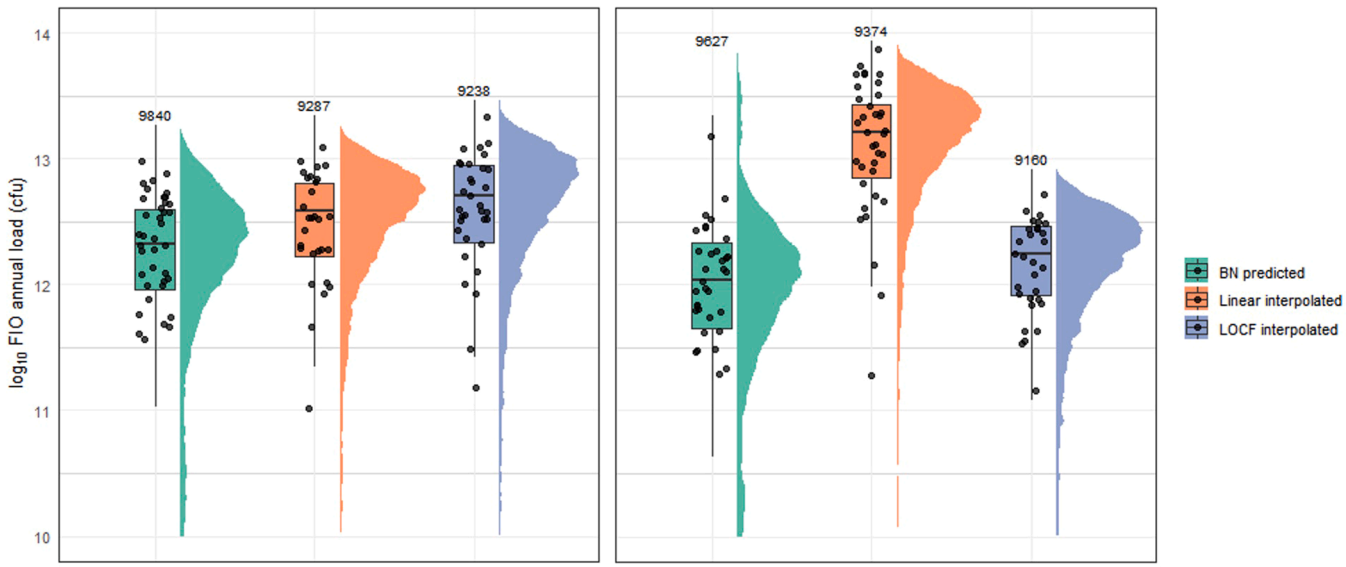

Fig. 4. Overall distribution of BN model predicted $\log_{10}$ FIO annual load (CFU) versus observed loads interpolated using the Last Observation Carried Forward and Linear interpolation methods in Cessnock (left) and Mein (right). BN predicted FIO loads are comparable to observed loads across both interpolation methods in Cessnock but under predict compared to Linear interpolated observed data in Mein. Outliers were excluded from the plots and the values above the boxplots show the number of samples plotted in each distribution. The distributions were plotted using the ggdist R package version 3.3.2.9000 (Kay 2024) with modified R code from Negri et al. (2024).

to STS with a high HOST-risk classification, at least 50 m from a watercourse, and a moderate slope (5–25 %). However, when the slope was gentler (0–5 %) under the same HOST and distance conditions, the FIO load dropped to 3.57×10^{10} cfu/year, showing a 15 % reduction due to slope effects.

Model uncertainty estimated through Shannon entropy was moderate to high (1.60–1.85) (Glendell et al., 2022), and was particularly high for STS where the predicted FIO load was low in Mein. These entropy values are between 71 % and 80 % of the maximum possible entropy (2.32[1]) for our target node which has 5 states (Vajapeyam, 2014). Although the BN predicted distribution of the realised FIO load is spread out as observed in Fig. 4, it is not completely uniform showing that the model still prefers certain states (medium to high FIO loads) in the target node. Further, the BN predicted distributions are comparable to the probability distributions of observed data.

Table 3

Fig. 6 illustrates heat maps displaying STS density and corresponding FIO load levels across Scotland. The eastern and central parts of Scotland have a high concentration of STS accounting for 32.9 % and 22.7 % respectively, of the 174,567 STS captured on the SEPA database (Fig. 6a). West Scotland has the lowest concentration accounting for 12.4 % while the South has 14.9 % and the North 17.2 %. Most STS with low (1,529) and moderate (22,515) HOST-derived risk factor are in East Scotland. Most STS with high HOST-derived risk factor are located in Central (29,893) and East Scotland (26,955). Most STS with very high HOST-derived risk factor are located in the East (6,365) and West regions (5,643). A table of STS counts and HOST-derived risk factors by regions is available in the Supplementary materials. While Aberdeenshire has a high STS density, a significant proportion generate an FIO load below the median as observed from the clustering of weighted points visualised by deep blue shading in Fig. 6b & c. In total, six local authority areas (LAs) in East and South Scotland out of 32 have been identified as high-risk zones for FIO pollution from STS (Fig. 6d). These areas combine a high STS density with FIO loads exceeding the median. Ayrshire and East Renfrewshire show the highest risk, as highlighted in Fig. 6e, where deep red shading represents STS with FIO loads above the third quartile.

4. Discussion

Validating model predictions with observed data is essential to demonstrate a model's appropriateness for its intended use and to foster trust in its outcomes. Our study successfully validated, for the first time, a BN model designed to characterise FIO losses from STS in rural catchments. Here, we discuss our findings in four key areas: (1) novel contributions of the research; (2) landscape features impacting FIO pollution from STS; (3) uncertainty and variability in model predictions, alongside implications from sensitivity analysis; (4) model transferability to other regions and from catchment to national scale, and potential policy interventions.

Our research is the first to show how BN models can predict FIO pollution from STS to watercourses. Other research utilising BNs to investigate FIO pollution of water has focused on sources such as recycled water (Donald et al., 2009), sewer outflows (Goulding et al., 2012) and other matrices such as submerged aquatic vegetation (SAV), sediments, and stormwater (Staley et al., 2012). We have thus contributed unique insight into understanding FIO pollution from STS by using a BN model to integrate diverse data types, such as expert opinion (Mzyece et al., 2024), modelled locations of STS from SEPA, and STS FIO concentration data (Kay et al., 2008). This approach not only enabled effective model predictions when challenged with gaps in data but also facilitated model validation—an area where BNs based entirely on expert knowledge face challenges (Constantinou et al., 2016; Kleemann et al., 2017). By deploying a hybrid and discrete BN to quantify information loss due to discretization we have addressed concerns raised in prior research (Aguilera et al., 2010; Glendell et al., 2022). In addition, our use of two interpolation methods ensured a robust methodology (Lepot et al., 2017), with better validation outcomes observed when using LOCF over linear interpolation, avoiding significant underprediction. Furthermore, our study explored FIO pollution in relation to a combination of landscape factors at a catchment scale, contributing new knowledge beyond previous studies that focused on individual factors considered in isolation, such as soil properties at laboratory scale (Billian et al., 2018) or STS proximity to watercourses at a watershed

[1] Maximum entropy calculated as $H_{max} = log_2\ (5)$ where 5 is the number of states in the target node.

Table 2
Predicted and observed FIO load per STS and load per catchment from the hybrid and discrete models.

			Predicted Total FIO load per catchment from hybrid BN	Total FIO load per catchment from equal intervals discretised BN	Total FIO load per catchment from interpolated discretised BN	FIO load per STS from hybrid BN	FIO load per STS from equal intervals discretised BN	FIO load per STS from interpolated discretised BN	Observed Total FIO load per catchment from Linear interpolation method	Total FIO load per catchment from LOCF interpolation method	FIO load per STS
Cessnock	Mean	cfu/yr	2.76×10^{12}	–	–	4.63×10^{10}	3.59×10^{10}	3.85×10^{10}	4.05×10^{12}	5.55×10^{12}	6.17×10^{10}
	Median		2.04×10^{12}	–	–	3.22×10^{10}	3.25×10^{10}	3.6×10^{10}	3.47×10^{12}	4.58×10^{12}	5.25×10^{10}
	Sum		–	2.34×10^{12}	2.50×10^{12}	–	–	–	–	–	–
	Minimum		2.09×10^{9}	–	–	–	–	–	6.18×10^{-15}	8.32×10^{-19}	–
	5th quantile		8.61×10^{11}	–	–	–	–	–	1.25×10^{12}	1.51×10^{12}	–
	75th quantile		3.88×10^{12}	–	–	–	–	–	6.15×10^{12}	8.52×10^{12}	–
	Maximum		1.84×10^{13}	–	–	–	–	–	2.22×10^{13}	2.90×10^{13}	
	SD		2.48×10^{12}			4.85×10^{10}	5.42×10^{9}	3.87×10^{9}	3.37×10^{12}	4.8×10^{12}	5.14×10^{10}
	PBIAS	%	–	–	–	–	–	–	−41.21	−55.46	–
	Under		–	–	–	–	–	–	45	52	–
	Optimal		–	–	–	–	–	–	25	22	–
	Over		–	–	–	–	–	–	30	26	–
	Shannon entropy		–	–	–	–	1.26	1.62	–	–	–
Mein	Mean	cfu/yr	2.31×10^{12}	–	–	4.36×10^{10}	3.32×10^{10}	3.65×10^{10}	1.74×10^{13}	1.85×10^{12}	5.10×10^{10}
	Median		1.04×10^{12}	–	–	2.86×10^{10}	3.57×10^{10}	3.10×10^{10}	1.49×10^{13}	1.58×10^{12}	4.34×10^{10}
	Sum		–	1.31×10^{12}	1.16×10^{12}	–	–	–	–	–	–
	Minimum		2.23×10^{8}	–	–	–	–	–	1.76×10^{-10}	1.64×10^{-23}	–
	5th quantile		3.85×10^{11}	–	–	–	–	–	5.26×10^{12}	5.64×10^{11}	–
	75th quantile		2.09×10^{12}	–	–	–	–	–	2.63×10^{13}	2.81×10^{12}	–
	Maximum		7.25×10^{13}	–	–			–	8.72×10^{13}	8.24×10^{12}	–
	SD		1.38×10^{12}			4.82×10^{10}	4.48×10^{9}	5.12×10^{9}	1.44×10^{13}	1.55×10^{12}	4.28×10^{10}
	PBIAS	%	–	–	–	–	–	–	−93.02	−34.18	–
	Under		–	–	–	–	–	–	83	42	–
	Optimal		–	–	–	–	–	–	5	25	–
	Over		–	–	–	–	–	–	12	33	–
	Shannon entropy		–	–	–	–	1.26	1.62	–	–	–

scale (Sowah et al., 2014). Limited research, whether empirical or modelled, exists on the combined effect of landscape factors on FIO transfer from STS to watercourses.

Our BN model combined three critical landscape factors: HOST-derived effluent movement risk, slope, and proximity to watercourses. The effluent movement risk provides an integrated assessment for surface runoff, groundwater leaching and the presence/absence of groundwater within 2 m depth as key FIO transfer pathways (Glendell et al., 2021). According to our BN model, the risk of FIO transfer is exacerbated by steep slopes and shorter distances to watercourses, which complements understanding of FIO transfer dynamics informed by both reductionist approaches using replicated soil boxes (Hodgson et al., 2016) and empirical field observations (Oliver et al., 2015; Srinivasan et al., 2021).

The riskiest combination of landscape features resulting in the highest STS FIO load (4.8×10^{10} cfu/yr) to a watercourse was very high HOST-derived risk classification, medium slope (5–25 %) and STS distance to a watercourse of ≥50 m. Here, both surface runoff (where soils are peaty or a shallow gleyed layer is present that inhibits drainage) and leaching to groundwater (where soils are free draining and an aquifer is also normally present within 2 m), are possible pollution pathways (Gagkas and Lilly, 2019). In contrast, the lowest FIO load of 1.22×10^{10} cfu/yr was generated from STS in soils with a low HOST-based risk classification, moderate slope and STS distance to a watercourse of >50 m. These areas featured relatively free-draining soils, no gleyed layer within 1 m, and no significant aquifer or groundwater. Here, the absence of an aquifer or groundwater contributed to low risk by preventing FIOs from reaching groundwater and later surface water via subsurface pathways (Buckerfield et al., 2019). Although some surface runoff is likely in soils with this HOST-derived classification, gentle slopes can reduce surface runoff resulting in water ponding and subsequently there might be increased FIO losses through leachate (Appels et al., 2016). For STS in soils with medium HOST-based risk —characterised by slow permeability within 1 m or gleying at 0.4 to 1 m and groundwater normally present at >2 m depth, the FIO load reaching a watercourse was slightly higher (3.7×10^{10} cfu/yr) compared to the previous scenario. This increase is likely due to greater FIO losses through surface runoff over the gleyed layer, as well as the influence of moderate slopes

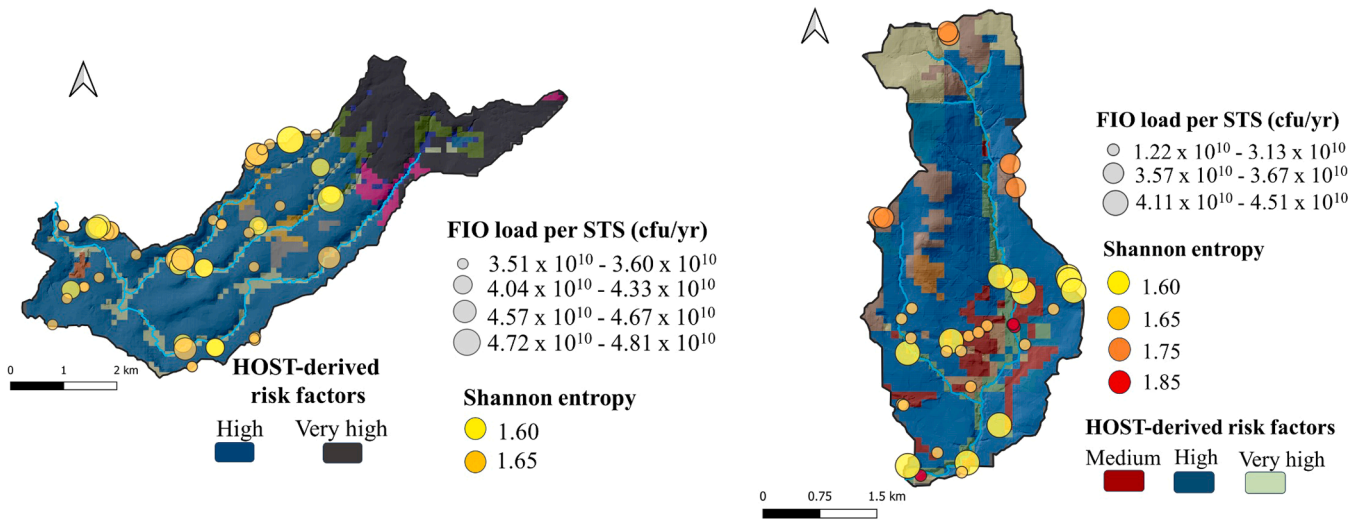

Fig. 5. Predicted FIO load per septic tank in Cessnock (left) and Mein (right). Circle size indicates the magnitude of the load, with smaller circles denoting lower FIO loads and larger circles indicating higher loads. Circle colour reflects entropy levels. The background map shows the HOST-derived risk factors. Note that the scale used to depict the predicted FIO load differs between the two catchments.

Table 3
Summary information relating to the sensitivity of each node.

Node	Sensitivity		
	Minimum	Maximum	Average
Treatment	0	0.478	0.200
Condition	0	0.450	0.194
Direct discharge	0	0.181	0.084
ST_concentration	0	0.521	0.049
STload	0	0.328	0.028
HOST_risk	0	0.091	0.029
ST_distance	0	0.037	0.014
Slope	0	0.014	0.005
FIO delivery	0	0.032	0.001
Realised STload	0	0.133	0.003

(5–25 %), which enhance FIO transport via surface runoff.

While a moderate slope can increase the FIO load to a watercourse by promoting surface runoff, the proximity of an STS to a watercourse plays a more significant role. This is evident in the higher FIO load increase (23 %) observed when the distance between the STS and the watercourse is reduced from 50 m to 10–50 m, compared to a 13 % increase associated with a slope change from 0 to 5 % to 5–25 %. These results are reinforced by the findings of Mzyece et al. (2024) where experts judged that the proportion of FIOs from a STS reaching a watercourse would increase by 20 % if the STS was located 10–50 m to a watercourse compared to 9 % if it was located >50 m from the watercourse. The greater FIO load due to reduced distance is attributed to fewer environmental barriers intercepting the STS effluent before it reaches the watercourse. For example, Stall et al. (2014), found that for STS effluent moving in an unsaturated zone of sandy soil via matrix flow, 30–45 cm to the groundwater table was less effective in straining bacterial colloids from the effluent and preventing groundwater pollution while 60 cm proved to be more effective. A similar principle applies to STS effluent transport to surface water and highlights the importance of maintaining a minimum 10 m buffer between an STS discharge and the nearest watercourse if not used as a drinking water source (SEPA, 2025). Longer distances, ranging from 50 m to 1.5 km, may be required depending on: the number of properties connected to the STS; whether it includes a soakaway; and the presence of a drinking water source in the area.

Although guidelines on appropriate slopes for STS placement are limited, UK construction standards implemented by the National Housing Building Council recommend slopes no steeper than 2 % for inflow connections to STS, to reduce influent velocity and disturbance in the tank, and no steeper than 0.5 % for effluent pipes in drain fields, to allow for extended retention and effective treatment. Our study further advises that STS planned for locations approximately 10 m from a watercourse should be constructed on slopes not exceeding 5 %. This approach can minimize runoff and reduce FIO loads by up to 13 %, compared to systems built on steeper slopes of 5–25 %.

Our study did not investigate the wider impact of land cover, e.g., improved grasslands, on water quality because this was beyond our scope. However, this topic has been addressed using the SCIMAP model, which demonstrated that variations in land management practices and coverage can affect FIO transfer within catchments (Porter et al., 2017). Typically, rural catchments with extensive grassland cover are more likely to experience animal-derived FIO pollution from agricultural applications of manure and slurries, livestock faeces and human FIO pollution from STS (Hodgson et al., 2016; Oliver et al., 2018; Richards et al., 2016). Therefore, of crucial importance to our model evaluation was a need to differentiate between human sources of FIOs and those contributed via agricultural practices. We capitalised on the availability of accompanying MST data collected within our test catchments, which allowed us to distinguish between human and livestock FIO pollution signals in surface water and in turn deliver credible predictions of FIO loads contributed from STS in rural catchments. The integration of MST data with modelling results is increasing and can provide an effective approach to help differentiate sources of other pollutants in catchments too, for example nitrogen (Zimmer-Faust et al., 2025)

The BN model's ability to predict mean and median values in the same order of magnitude as the observed data demonstrates that our model is fit for purpose (Neill et al., 2020). It assigned risk of FIO pollution from STS based on STS condition, location and the additional effects of landscape features in either reducing or increasing FIO transfer to waterbodies. However, the model underpredicted FIO loads, potentially due to overestimated treatment levels or the proportion of well-maintained STS (Glendell et al., 2021). Observed data limitations, such as seasonal sampling biases, may have also contributed to discrepancies (Sorensen et al., 2021; Torres et al., 2022) since in-stream FIO data are scarce, in part because the UK does not routinely monitor all rivers for microbial pollution (Oliver et al., 2016). Accessing good quality long-term data for model testing can therefore be challenging.

We were able to access FIO data collected over an annual period by SEPA; however, one year of data cannot capture the full range of hydrological variability likely to influence uncertainty of observations. The

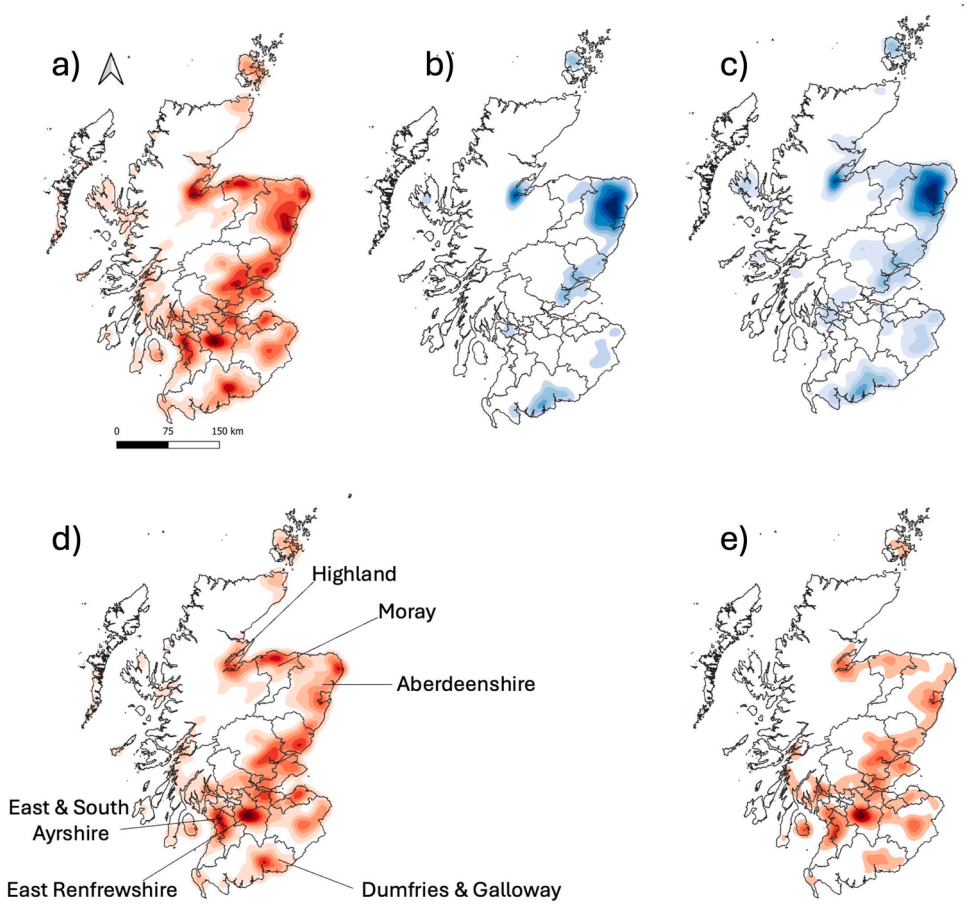

Fig. 6. Heatmaps visualising: a. STS density calculated using kernel density estimation with high density represented by deep red colour shading and lower density represented by light shading. The points representing STS are weighted as follows: b. STS with FIO load less than Q1 (5.60×10^{10} cfu/yr); c. STS with FIO load less than the Median (7.88×10^{10} cfu/yr); d. STS with FIO load greater than the Median (7.88×10^{10} cfu/yr) and e. STS with FIO load greater than the Q3 (9.13×10^{10} cfu/yr). The black lines in the maps represent boundaries of local authority areas in Scotland.

dataset comprised twice-weekly 24-h composite samples—an unusually high sampling frequency. For comparison, McDowell et al. (2024) suggest that twice-monthly sampling can be sufficient to detect long-term water quality trends and inform policy. Nonetheless, gaps within the twice-weekly design may not fully capture seasonal and flow variability affecting FIO mobilisation. For example, human FIO loads observed in summer to early autumn (September to November) are likely to be high due to nearby terrestrial sources benefitting from warmer temperatures (Cho et al., 2010) and therefore not representative of year-round conditions. Our accompanying MST data also represents a point in time for each sample and therefore, may not accurately represent the dynamic changes in human/livestock proportions, as influenced by seasonality and temporal factors (Ahmed et al., 2013; Duncan et al., 2013). While such factors can be critical when estimating absolute diffuse-source FIO loads, this study's aim was to evaluate a model of septic tank inputs. Observed load estimates were used primarily as a "sense check" to confirm that model predictions did not exceed plausible catchment-scale loads.

Interpolation can introduce uncertainty, particularly when data gaps are large. LOCF often underestimates variability and can overemphasise a sample collected immediately before a pause in sampling, potentially skewing the inferred daily load if conditions at that time were atypical (Mavridis et al., 2019). To address this, we also applied linear interpolation, which assumes a constant rate of change between observations and reduces—but does not remove—bias under changing conditions (Juhan et al., 2025). The use of both approaches provides a range of plausible load estimates, serving as a safeguard against unrealistic predictions rather than as a definitive quantification of total load. Future work could test the model in even more data-rich catchments if supported by targeted sampling campaigns —ideally with little or no wastewater treatment influence—paired with high-resolution FIO sampling to better capture the full range of water quality dynamics.

Our BN model generally exhibited high uncertainty, particularly when predicting low FIO loads. This indicated lower confidence in assessing low-risk scenarios compared to high-risk ones. This discrepancy may have been due to a data imbalance (Fanconi et al., 2023), as fewer STS exhibited low FIO loads (8 % in Mein) compared to the majority (92 %) showing medium to high loads. As a result, the BN model was better trained to recognize high FIO load patterns (Lambert et al., 2022). Furthermore, the limited data on the condition and maintenance of STS with low FIO loads increased prediction uncertainty. To reduce this uncertainty, high-quality data on STS condition and maintenance—identified as critical parameters through sensitivity analysis (Kaikkonen et al., 2020)—are needed. Therefore, future research should prioritize gathering more reliable data on STS condition and maintenance, including targeted surveys of septic tank owners to gain insight into their system management practices and perceptions of STS-related risks.

Uncertainty analysis also provided valuable insights into the model's transferability with respect to soil and hydrological characteristics. BN application to areas with relatively homogeneous soil hydrological characteristics resulted in greater confidence in modelled outputs. However, BN predictions were susceptible to increased uncertainty when applied in a catchment with diverse soil-hydrological

characteristics. As catchments become larger and more complex, whether due to underlying soil, hydrological and geological characteristics or because of greater diversity and nuance in land use or management approaches, we can expect model predictions to be accompanied with higher uncertainty, and this is not uncommon (Boodoo et al., 2025; Woodward et al., 2017; Yao et al., 2025). Therefore, when the BN was applied to the national scale STS data for Scotland, greater confidence in model results was associated with Central, East and West Scotland where most STS i.e. 29,873, 26,955 and 17,051 respectively, were associated with a moderate to high HOST-derived risk classification. In contrast, predictions were more uncertain for South Scotland, which featured STS associated with a variability of HOST-derived risk factors. Here, the model predictions can be utilised as a first approximation of FIO water pollution risk from STS, helping to prioritise spatial investigation on-the-ground, recognising that further data input on the condition/maintenance of STS would help to improve model outcomes.

The model offers further critical insight into areas in Scotland at high risk of FIO pollution from STS, particularly rural and agricultural regions where livestock-driven FIO pollution has been widely studied (Neill et al., 2018; Oliver et al., 2016; Scottish Government RESAS, 2017). In rural agricultural catchments, STS are rarely considered in terms of their overall contribution to the FIO load of receiving waters, in part because they are challenging to monitor and due to difficulties in differentiating the human/livestock FIO signal (Diaz-Elsayed et al., 2017; Harwood et al., 2013). To date, greater emphasis has been given to understanding the relative importance of different agricultural sources of FIOs, (e.g. Hodgson et al., 2016; Murphy et al., 2015; Neill et al., 2020; Oliver et al., 2018; Zimmer-Faust et al., 2025), and more recently wildlife contributions (Afolabi et al., 2020). Therefore, the development of tools and modelling approaches, built on credible evidence as demonstrated in our study, helps to identify the contribution of STS is essential to ensure these sources are not overlooked.

Using Scotland as a case study, our findings highlight that a high density of STS does not necessarily translate to high FIO loading of receiving waters, as observed for northeast Scotland, where risks appear to be well constrained. In contrast, southwest Scotland contributed higher FIO loads from STS and exceeded the 3rd quartile, which is significantly higher than the EU bathing water standards for inland waters and therefore a cause for concern. Indeed, bathing water quality in some areas across SW Scotland has been of lower quality relative to other bathing waters in Scotland (Scottish Environment Protection Agency, 2016). This is often attributed to intensive dairy farming and wetter weather (Edwards et al., 2008; Vinten et al., 2008); however, our findings raise the prospect that STS contributions to FIO loading of receiving waters may also play an important role in influencing microbial pollution in this region of Scotland.

5. Conclusion

To our knowledge, this is the first time a BN model has been shown to effectively predict FIO losses from STS to watercourses in rural catchments, demonstrating how STS condition and maintenance influence FIO loads. Additionally, our approach highlights how soil hydrology, slope, and the distance between the STS and watercourses either hinder or facilitate FIO transfer from STS to receiving waters. The multi-scale application of the BN model from catchment to national scale further demonstrates its use and value to policy-makers and land managers with a responsibility for water quality assessment. Enhancing model performance especially in catchments with varied soil-hydrological characteristics, will require future research to refine data on STS condition and maintenance while validating model predictions with high-resolution and longer-term data. Improved data will not only enhance model accuracy but also aid regulators and researchers in understanding septic tank users' perceptions of faecal pollution risks to watercourses. Ultimately, this BN model demonstrates a crucial step in developing a tool that regulators can use to mitigate pollution from often-overlooked sources such as STS, thus contributing to further safeguarding of bathing water quality and public health. Expanding the BN model framework to account for a wider range of FIO sources typical of more complex mixed land use catchments represents an important next step. This would help to improve holistic assessment of FIO contributions from diffuse agricultural sources, municipal wastewater effluent discharges and wildlife, in addition to STS.

Institutional review board statement

Ethical approval for the project was granted by the University of Stirling, General University Ethics Panel.

Declaration of generative AI and AI-assisted technologies in the writing process

During the preparation of this work the author used ChatGPT to improve readability of selected sections of the manuscript. After using this tool/service, the author reviewed and edited the content as needed and take full responsibility for the content of the publication.

Funding

This study was conducted as part of a PhD funded by the UK Commonwealth Scholarship Commission awarded under the theme Science and Technology for Development.

CRediT authorship contribution statement

Chisha Chongo Mzyece: Writing – review & editing, Writing – original draft, Visualization, Project administration, Methodology, Investigation, Funding acquisition, Formal analysis, Data curation, Conceptualization. **Miriam Glendell:** Writing – review & editing, Validation, Supervision, Software, Methodology, Investigation, Formal analysis, Data curation, Conceptualization. **Zisis Gagkas:** Writing – review & editing, Software, Formal analysis, Data curation. **Mads Troldborg:** Writing – review & editing, Software, Methodology, Formal analysis. **Camilla Negri:** Software, Formal analysis. **Eulyn Pagaling:** Methodology, Data curation. **Ian Jones:** Supervision, Conceptualization. **David M. Oliver:** Writing – review & editing, Validation, Supervision, Methodology, Investigation, Formal analysis, Conceptualization.

Declaration of competing interest

The authors declare no conflict of interest. The funders had no role in the design of the study; in the collection, analyses, or interpretation of data; in the writing of the manuscript, or in the decision to publish the results.

Acknowledgement

The authors wish to acknowledge staff at SEPA for their valuable contribution to this research: Susan Campbell for providing the FIO monitoring data for the Cessnock and Mein catchments. Special thanks to Brian McCreadie from SEPA for facilitating access to the data and Ruth Stidson from SEPA for contributing constructive ideas in the initial stages of the research.

Supplementary materials

Supplementary material associated with this article can be found, in the online version, at doi:10.1016/j.watres.2025.124715.

Data availability

Data will be made available on request.

References

Afolabi, E.O., Quilliam, R.S., Oliver, D.M., 2020. Impact of freeze–thaw cycles on die-off of *E. coli* and intestinal enterococci in deer and dairy faeces: implications for landscape contamination of watercourses. Int. J. Environ. Res. Public Health 17 (19), 1–16. https://doi.org/10.3390/ijerph17196999.

African Development Bank, 2020. *Sanitation and Wastewater Atlas of Africa*. African Development Bank. Water Development and Sanitation Department; United Nations Environment Programme; GRID-Arendal.

Aguilera, P.A., Fernández, A., Fernández, R., Rumí, R., Salmerón, A., 2011. Bayesian networks in environmental modelling. Environ. Model. Softw. 26 (12), 1376–1388. https://doi.org/10.1016/j.envsoft.2011.06.004.

Aguilera, P.A., Fernández, A., Reche, F., Rumí, R., 2010. Hybrid Bayesian network classifiers: application to species distribution models. Environ. Model. Softw. 25 (12), 1630–1639. https://doi.org/10.1016/j.envsoft.2010.04.016.

Ahmed, W., Sritharan, T., Palmer, A., Sidhu, J.P.S., & Toze, S. (2013). *Evaluation of Bovine Feces-Associated Microbial Source Tracking Markers and Their Correlations with Fecal Indicators and Zoonotic Pathogens in a Brisbane, Australia, Reservoir*. https://doi.org/10.1128/AEM.03234-12.

Appels, W.M., Bogaart, P.W., van der Zee, S.E.A.T.M., 2016. Surface runoff in flat terrain: how field topography and runoff generating processes control hydrological connectivity. J. Hydrol. 534, 493–504. https://doi.org/10.1016/j.jhydrol.2016.01.021.

Appling, D., Habteselassie, M.Y., Radcliffe, D., Bradshaw, J.K., 2013. Preliminary study on the effect of wastewater storage in septic tank on *E. coli* concentration in summer. Water 5 (3), 1141–1151. https://doi.org/10.3390/w5031141.

BayesFusion, L., 2024. https://support.bayesfusion.com/docs/.

Beal, C.D., Gardner, E.A., Menzies, N.W., 2005. Process, performance, and pollution potential: a review of septic tank–soil absorption systems. Soil. Res. 43 (7), 781–802. https://doi.org/10.1071/SR05018.

Beuzen, T., Marshall, L., Splinter, K.D., 2018. A comparison of methods for discretizing continuous variables in Bayesian Networks. Environ. Model. Softw. 108, 61–66. https://doi.org/10.1016/j.envsoft.2018.07.007.

Billian, H., Krometis, L.A., Thompson, T., Hagedorn, C., 2018. Movement of traditional fecal indicator bacteria and source-tracking targets through septic drainfields. Sci. Total. Environ. 610–611, 1467–1475. https://doi.org/10.1016/j.scitotenv.2017.08.131.

Boodoo, F., Hostache, R., Skifa, N., Guerin, J., Delenne, C., 2025. Are LSTM and conceptual rainfall-runoff models able to cope with limited training datasets under diverse hydrometeorological conditions? Model. Earth. Syst. Environ. 11 (2). https://doi.org/10.1007/s40808-025-02316-z.

Bradford, S.A., Harvey, R.W., 2017. Future research needs involving pathogens in groundwater. Hydrogeol. J. 25 (4), 931–938. https://doi.org/10.1007/s10040-016-1501-0.

Buckerfield, S.J., Quilliam, R.S., Waldron, S., Naylor, L.A., Li, S., Oliver, D.M., 2019. Rainfall-driven *E. coli* transfer to the stream-conduit network observed through increasing spatial scales in mixed land-use paddy farming karst terrain. Water. Res. X. 5. https://doi.org/10.1016/j.wroa.2019.100038.

Cassidy, R., Jordan, P., Bechmann, M., Kronvang, B., Kyllmar, K., Shore, M., 2018. Assessments of composite and discrete sampling approaches for water quality monitoring. Water Resour. Manag. 32 (9), 3103–3118. https://doi.org/10.1007/s11269-018-1978-5.

Chen, S.H., Pollino, C.A., 2012. Good practice in Bayesian network modelling. Environ. Model. Softw. www.bayesia.com.

Cho, K.H., Cha, S.M., Kang, J.H., Lee, S.W., Park, Y., Kim, J.W., Kim, J.H., 2010. Meteorological effects on the levels of fecal indicator bacteria in an urban stream: a modeling approach. Water. Res. 44 (7), 2189–2202. https://doi.org/10.1016/j.watres.2009.12.051.

Constantinou, A.C., Fenton, N., Neil, M., 2016. Integrating expert knowledge with data in Bayesian networks: preserving data-driven expectations when the expert variables remain unobserved Europe PMC Funders Group. Expert. Syst. Appl. 56, 197–208. https://doi.org/10.1016/j.eswa.2016.02.050.

Defra. (2002). *Sewage Treatment in the UK Implementation of the EC Urban Wastewater Treatment Directive*.

Diaz-Elsayed, N., Xu, X., Balaguer-Barbosa, M., Zhang, Q., 2017. An evaluation of the sustainability of onsite wastewater treatment systems for nutrient management. Water. Res. 121, 186–196. https://doi.org/10.1016/j.watres.2017.05.005.

Donald, M., Cook, A., Mengersen, K., 2009. Bayesian network for risk of diarrheal associated with the use of recycled water. Risk. Anal. 29 (12), 1672–1685. https://doi.org/10.1111/j.1539-6924.2009.01301.x.

Duncan, J.S., Leatherbarrow, A.J.H., French, N.P., & Grove-White, D.H. (2013). *Temporal and farm-management-associated variation in faecal-pat prevalence of Campylobacter fetus in sheep and cattle*. https://doi.org/10.1017/S0950268813002379.

Edwards, A.C., Kay, D., McDonald, A.T., Francis, C., Watkins, J., Wilkinson, J.R., Wyer, M.D., 2008. Farmyards, an overlooked source for highly contaminated runoff. J. Environ. Manag. 87 (4), 551–559. https://doi.org/10.1016/j.jenvman.2006.06.027.

Ellerman, D., 2021. The relationship between logical entropy and Shannon entropy. New Foundations for Information Theory. Springer, Cham, pp. 15–22. https://doi.org/10.1007/978-3-030-86552-8_2.

Fanconi, C., De Hond, A., Peterson, D., Capodici, A., Hernandez-Boussard, T., 2023. A Bayesian approach to predictive uncertainty in chemotherapy patients at risk of acute care utilization. https://github.com/su.

Fenton, N., Neil, M., 2018. *Risk assessment and decision analysis with Bayesian networks*. Crc Press.

Feutrill, A., Roughan, M., 2021. A review of shannon and differential entropy rate estimation. Entropy. MDPI AG. https://doi.org/10.3390/e23081046 (Vol. 23, Issue 8).

Gagkas, Z., Lilly, A., 2019. Downscaling soil hydrological mapping used to predict catchment hydrological response with random forests. Geoderma 341, 216–235. https://doi.org/10.1016/j.geoderma.2019.01.048.

Gagkas, Z., Lilly, A., Baggaley, N.J., 2021. Digital soil maps can perform as well as large-scale conventional soil maps for the prediction of catchment baseflows. Geoderma 400. https://doi.org/10.1016/j.geoderma.2021.115230.

Gill, L.W., O'Súlleabháin, C., Misstear, B.D.R., Johnston, P.J., 2007. The treatment performance of different subsoils in Ireland receiving on-site wastewater effluent. J. Environ. Qual. 36 (6), 1843–1855. https://doi.org/10.2134/jeq2007.0064.

Glendell, M., Gagkas, Z., Richards, S., & Halliday, S. (2021). *Developing a probabilistic risk model to estimate phosphorus, nitrogen and microbial pollution to water from septic tanks full report*.

Glendell, M., Gagkas, Z., Stutter, M., Richards, S., Lilly, A., Vinten, A., Coull, M., 2022. A systems approach to modelling phosphorus pollution risk in Scottish rivers using a spatial Bayesian belief network helps targeting effective mitigation measures. Front. Environ. Sci. 10. https://doi.org/10.3389/fenvs.2022.976933.

Goulding, R., Jayasuriya, N., Horan, E., 2012. A Bayesian network model to assess the public health risk associated with wet weather sewer overflows discharging into waterways. Water. Res. 46 (16), 4933–4940. https://doi.org/10.1016/j.watres.2012.03.044.

Harwood, V.J., Boehm, A.B., Sassoubre, L.M., Vijayavel, K., Stewart, J.R., Fong, T.T., Caprais, M.P., Converse, R.R., Diston, D., Ebdon, J., Fuhrman, J.A., Gourmelon, M., Gentry-Shields, J., Griffith, J.F., Kashian, D.R., Noble, R.T., Taylor, H., Wicki, M., 2013. Performance of viruses and bacteriophages for fecal source determination in a multi-laboratory, comparative study. Water. Res. 47 (18), 6929–6943. https://doi.org/10.1016/j.watres.2013.04.064.

Hodgson, C.J., Oliver, D.M., Fish, R.D., Bulmer, N.M., Heathwaite, A.L., Winter, M., Chadwick, D.R., 2016. Seasonal persistence of faecal indicator organisms in soil following dairy slurry application to land by surface broadcasting and shallow injection. J. Environ. Manag. 183, 325–332. https://doi.org/10.1016/j.jenvman.2016.08.047.

Hojsgaard, S., 2012. Graphical independence networks with the gRain package for R. J. Stat. Softw. 46 (10), 1–26. https://doi.org/10.18637/jss.v046.i10.

Hudson, G., Lilly, A., Higgins, A.J., Jordan, C., Fealy, R., Creamer, R.E., & Hutton Institute, J.-J. (2012). *D4.3 GS soil test case report: Celtic Fringe of Europe <D4.3 data harmonization Best practice guidelines>test case report: harmonisation of 1:250 000 scale soil maps and soil profile data in the Celtic Fringe of Europe: Scotland, Northern Ireland and Eire deliverable number dissemination level*.

Jensen, F., 1996. An Introduction to Bayesian Networks. UCL Press.

Juhan, N., Jamaludin, S.N., Zubairi, Y.Z., Ag Isha, D.S.N.S., Khaliludin, N.I.A., 2025. Comparative analysis of imputation methods for missing environmental data: a case study on ozone concentrations. J. Adv. Res. Des. 134 (1), 63–76. https://doi.org/10.37934/ard.134.1.6376.

Kaikkonen, L., Parviainen, T., Rahikainen, M., Uusitalo, L., Lehikoinen, A., 2020. Bayesian networks in environmental risk assessment: a review. Integr. Environ. Assess. Manag. 17 (1), 62–78. https://doi.org/10.1002/ieam.4332.

Kay, D., Crowther, J., Stapleton, C.M., Wyer, M.D., Fewtrell, L., Edwards, A., Francis, C. A., McDonald, A.T., Watkins, J., Wilkinson, J., 2008. Faecal indicator organism concentrations in sewage and treated effluents. Water. Res. 42 (1–2), 442–454. https://doi.org/10.1016/j.watres.2007.07.036.

Kay, M., 2024. Ggdist: visualizations of distributions and uncertainty in the grammar of graphics. IEEE Trans. Vis. Comput. Graph. 30 (1), 414–424. https://doi.org/10.1109/TVCG.2023.3327195.

Kildare, B.J., Leutenegger, C.M., McSwain, B.S., Bambic, D.G., Rajal, V.B., Wuertz, S., 2007. 16S rRNA-based assays for quantitative detection of universal, human-, cow-, and dog-specific fecal bacteroidales: a bayesian approach. Water. Res. 41 (16), 3701–3715. https://doi.org/10.1016/j.watres.2007.06.037.

Kjaerulff, U., van der Gaag, L.C., 2000. Making sensitivity analysis computationally efficient. In: Uncertainty in Artificial Intelligence Proceedings.

Kleemann, J., Celio, E., Fürst, C., 2017. Validation approaches of an expert-based Bayesian belief network in Northern Ghana, West Africa. Ecol. Modell. 365, 10–29. https://doi.org/10.1016/J.ECOLMODEL.2017.09.018.

Lachin, J.M., 2016. Fallacies of last observation carried forward analyses. Clin. Trials 13 (2), 161–168. https://doi.org/10.1177/1740774515602688.

Lambert, B., Forbes, F., Tucholka, A., Doyle, S., Dehaene, H., Dojat, M., 2022. Trustworthy clinical AI solutions: a unified review of uncertainty quantification in deep learning models for medical image analysis. http://arxiv.org/abs/2210.03736.

Lepot, M., Aubin, J.B., Clemens, F.H.L.R., 2017. Interpolation in time series: an introductive overview of existing methods, their performance criteria and uncertainty assessment. Water 9 (10). https://doi.org/10.3390/w9100796. MDPI AG.

Madani, M., Seth, R., 2020. Evaluating multiple predictive models for beach management at a freshwater beach in the Great Lakes region. J. Environ. Qual. 49 (4), 896–908. https://doi.org/10.1002/jeq2.20107.

Marcot, B.G., Penman, T.D., 2019. Advances in Bayesian network modelling: integration of modelling technologies. Environ. Model. Softw. 111, 386–393. https://doi.org/10.1016/j.envsoft.2018.09.016. Elsevier Ltd.

Mavridis, D., Salanti, G., Furukawa, T.A., Cipriani, A., Chaimani, A., White, I.R., 2019. Allowing for uncertainty due to missing and LOCF imputed outcomes in meta-analysis. Stat. Med. 38 (5), 720–737. https://doi.org/10.1002/sim.8009.

McDowell, R.W., Noble, A., Kittridge, M., Ausseil, O., Doscher, C., Hamilton, D.P., 2024. Monitoring to detect changes in water quality to meet policy objectives. Sci. Rep. 14 (1), 1914. https://doi.org/10.1038/s41598-024-52512-7.

Moe, S.J., Carriger, J.F., Glendell, M., 2021. Increased use of Bayesian network models has improved environmental risk assessments. Integr. Environ. Assess. Manag 17 (1), 53–61. https://doi.org/10.1002/ieam.4369.

Morton, R.D., Marston, C.G., O'Neil, A.W., Rowland, C.S., 2024. Land cover Map 2023 (land parcels, GB) - EIDC. https://catalogue.ceh.ac.uk/documents/50b344eb-8343-423b-8b2f-0e9800e34bbd.

Murphy, S., Jordan, P., Mellander, P.E., O' Flaherty, V., 2015. Quantifying faecal indicator organism hydrological transfer pathways and phases in agricultural catchments. Sci. Total. Environ. 520, 286–299. https://doi.org/10.1016/j.scitotenv.2015.02.017.

Mzyece, C.C., Glendell, M., Gagkas, Z., Quilliam, R.S., Jones, I., Pagaling, E., Akoumianaki, I., Newman, C., Oliver, D.M., 2024. Eliciting expert judgements to underpin our understanding of faecal indicator organism loss from septic tank systems. Sci. Total. Environ. 921. https://doi.org/10.1016/j.scitotenv.2024.171074.

Negri, C., Schurch, N., Wade, A.J., Mellander, P.E., Stutter, M., Bowes, M.J., Glendell, M., 2024. Transferability of a Bayesian Belief Network across diverse agricultural catchments using high-frequency hydrochemistry and land management data. Sci. Total Environ. 949, 174926.

Neill, A.J., Tetzlaff, D., Strachan, N.J.C., Hough, R.L., Avery, L.M., Maneta, M.P., Soulsby, C., 2020. An agent-based model that simulates the spatio-temporal dynamics of sources and transfer mechanisms contributing faecal indicator organisms to streams. Part 2: application to a small agricultural catchment. J. Environ. Manag. 270. https://doi.org/10.1016/j.jenvman.2020.110905.

Neill, A.J., Tetzlaff, D., Strachan, N.J.C., Hough, R.L., Avery, L.M., Watson, H., Soulsby, C., 2018. Using spatial-stream-network models and long-term data to understand and predict dynamics of faecal contamination in a mixed land-use catchment. Sci. Total. Environ. 612, 840–852. https://doi.org/10.1016/j.scitotenv.2017.08.151.

Nojavan, F.A., Qian, S.S., Stow, C.A, 2017. Comparative analysis of discretization methods in Bayesian networks. Environ. Model. Softw. 87, 64–71. https://doi.org/10.1016/j.envsoft.2016.10.007.

OECD, 2023. Share of Resident Population Connected to an Urban Wastewater Treatment Point in Australia from 2010 to 2021. Statista.

O'keeffe, J., Akunna, J., Olszewska, J., Bruce, A., May, L., Allan, R., 2015. Practical measures for reducing phosphorus and faecal microbial loads from onsite wastewater treatment system discharges to the environment. A review. sepa.org.uk/media/163158/crew-septic-tanks.pdf.

Oliver, D.M., Bartie, P.J., Louise Heathwaite, A., Reaney, S.M., Parnell, J.A.Q., Quilliam, R.S., 2018. A catchment-scale model to predict spatial and temporal burden of *E. coli* on pasture from grazing livestock. Sci. Total. Environ. 616–617, 678–687. https://doi.org/10.1016/J.SCITOTENV.2017.10.263.

Oliver, D.M., Metcalf, R., Jones, D.L., Matallana-Surget, S., Thomas, D.N., Robins, P., Tulloch, C.L., Cotterell, B.M., Williams, G., Christie-Oleza, J.A., Quilliam, R.S., 2024. Plastic pollution and human pathogens: towards a conceptual shift in risk management at bathing water and beach environments. Water. Res. 261. https://doi.org/10.1016/j.watres.2024.122028. Elsevier Ltd.

Oliver, D.M., Porter, K.D.H., Louise Heathwaite, A., Zhang, T., Quilliam, R.S, 2015. Impact of low intensity summer rainfall on *E. coli*-discharge event dynamics with reference to sample acquisition and storage. Environ. Monit. Assess. 187 (7), 426. https://doi.org/10.1007/s10661-015-4628-x.

Oliver, D.M., Porter, K.D.H., Pachepsky, Y.A., Muirhead, R.W., Reaney, S.M., Coffey, R., Kay, D., Milledge, D.G., Hong, E., Anthony, S.G., Page, T., Bloodworth, J.W., Mellander, P.-E., Carbonneau, P.E., McGrane, S.J., Quilliam, R.S., 2016. Predicting microbial water quality with models: over-arching questions for managing risk in agricultural catchments. Sci. Total. Environ. 544, 39–47. https://doi.org/10.1016/J.SCITOTENV.2015.11.086.

Pearl, J., 2014. Probabilistic Reasoning in Intelligent systems: Network of Plausible Inference. Elsevier.

Phan, T.D., Smart, J.C.R., Capon, S.J., Hadwen, W.L., Sahin, O., 2016. Applications of Bayesian belief networks in water resource management: a systematic review. Environ. Model. Softw. 85, 98–111. https://doi.org/10.1016/j.envsoft.2016.08.006.

Pollino, C., & Henderson, C. (2010). *Bayesian networks: a guide for their application in natural resource management and policy*.

Porter, K.D., Reaney, S.M., Quilliam, R.S., Burgess, C., Oliver, D.M., 2017. Predicting diffuse microbial pollution risk across catchments: The performance of SCIMAP and recommendations for future development. Sci. Total Environ. 609, 456–465.

Price, R.G., Wildeboer, D., 2017. *E. coli* as an indicator of contamination and health risk in environmental waters. Escherichia Coli - Recent Advances On Physiology, Pathogenesis and Biotechnological Applications. InTech. https://doi.org/10.5772/67330.

QGIS Development Team, 2021. QGIS geographical information system. Open-Source Geospat. Found. https://qgis.org.

Reischer, G.H., Kasper, D.C., Steinborn, R., Mach, R.L., Farnleitner, A.H., 2006. Quantitative PCR method for sensitive detection of ruminant fecal pollution in freshwater and evaluation of this method in alpine karstic regions. Appl. Environ. Microbiol. 72 (8), 5610–5614. https://doi.org/10.1128/AEM.00364-06.

Richards, S., Paterson, E., Withers, P.J.A., Stutter, M., 2016. Septic tank discharges as multi-pollutant hotspots in catchments. Sci. Total. Environ. 542, 854–863. https://doi.org/10.1016/j.scitotenv.2015.10.160.

Rohmer, J., 2020. Uncertainties in conditional probability tables of discrete Bayesian Belief Networks: a comprehensive review. Eng. Appl. Artif. Intell. 88, 103384. https://doi.org/10.1016/J.ENGAPPAI.2019.103384.

Rossi, A., Wolde, B.T., Lee, L.H., Wu, M., 2020. Prediction of recreational water safety using *Escherichia coli* as an indicator: case study of the Passaic and Pompton rivers, New Jersey. Sci. Total. Environ. 714. https://doi.org/10.1016/j.scitotenv.2020.136814.

Sahlin, U., Helle, I., Perepolkin, D., 2020. "This is what we don't know": treating epistemic uncertainty in Bayesian networks for risk assessment. Integr. Environ. Assess. Manag. 17 (1), 221–232. https://doi.org/10.1002/ieam.4367.

Scottish Environment Protection Agency. (2016). *Scottish bathing waters 2016*.

Scottish Government RESAS, 2017. Agricultural maps for Scotland. www.gov.scot/publications/agriculture-maps/.

Scottish Water. (2025). *Scottish water reported overflow event data to SEPA 2020-2024*.

Scutari, M., 2010. Learning Bayesian networks with the bnlearn R package. J. Stat. Softw. 35 (3), 1–22. https://doi.org/10.18637/jss.v077.i02.

SEPA, 2025. Septic tanks and private sewage treatment systems. www.sepa.org.uk.

Seurinck, S., Defoirdt, T., Verstraete, W., Siciliano, S.D., 2005. Detection and quantification of the human-specific HF183 Bacteroides 16S rRNA genetic marker with real-time PCR for assessment of human faecal pollution in freshwater. Environ. Microbiol. 7 (2), 249–259. https://doi.org/10.1111/j.1462-2920.2004.00702.x.

Sorensen, J.P.R., Aldous, P., Bunting, S.Y., McNally, S., Townsend, B.R., Barnett, M.J., Harding, T., La Ragione, R.M., Stuart, M.E., Tipper, H.J., Pedley, S., 2021. Seasonality of enteric viruses in groundwater-derived public water sources. Water. Res. 207, 117813. https://doi.org/10.1016/J.WATRES.2021.117813.

Sowah, R., Zhang, H., Radcliffe, D., Bauske, E., Habteselassie, M.Y., 2014. Evaluating the influence of septic systems and watershed characteristics on stream faecal pollution in suburban watersheds in Georgia, USA. J. Appl. Microbiol. 117 (5), 1500–1512. https://doi.org/10.1111/jam.12614.

Sperotto, A., Molina, J.L., Torresan, S., Critto, A., Pulido-Velazquez, M., Marcomini, A., 2019. Water quality sustainability evaluation under uncertainty: a multi-scenario analysis based on bayesian networks. Sustainablity 11 (17). https://doi.org/10.3390/su11174764.

Srinivasan, M.S., Muirhead, R.W., Singh, S.K., Monaghan, R.M., Stenger, R., Close, M.E., Manderson, A., Drewry, J.J., Smith, L.C., Selbie, D., Hodson, R., 2021. Development of a national-scale framework to characterise transfers of N, P and *Escherichia coli* from land to water. N Z J. Agric. Res. 64 (3), 286–313. https://doi.org/10.1080/00288233.2020.1713822.

Staley, C., Reckhow, K.H., Lukasik, J., Harwood, V.J., 2012. Assessment of sources of human pathogens and fecal contamination in a Florida freshwater lake. Water. Res. 46 (17), 5799–5812. https://doi.org/10.1016/j.watres.2012.08.012.

Stall, C., Amoozegar, A., Lindbo, D., Graves, A., 2014. Transport of *E. coli* in a Sandy soil as impacted by depth to water table. J. Environ. Health 76 (6), 92–101. https://doi.org/10.2307/26329962.

Torres, C., Gitau, M.W., Paredes-Cuervo, D., Engel, B., 2022. Evaluation of sampling frequency impact on the accuracy of water quality status as determined considering different water quality monitoring objectives. Environ. Monit. Assess. 194 (7), 1–23. https://doi.org/10.1007/S10661-022-10169-7/METRICS.

Troldborg, M., Gagkas, Z., Vinten, A., Lilly, A., Glendell, M., 2021. Probabilistic modelling of inherent field-level pesticide pollution risk in a small drinking water catchment using Bayesian Belief Networks. Hydrol. Earth Syst. Sci. Discuss. 1–44.

USEPA. (2021). *Report to Congress on the prevalence throughout the U.S. of low- and moderate-income households without access to a treatment works and the use by states of assistance under section 603(c)(12) of the Federal Water Pollution Control Act*.

Vajapeyam, S. (2014). *Understanding Shannon's entropy metric for information*.

Van Rossum, G., Drake, F.L., 2009. Python 3 Reference Manual. CreateSpace.

Vinten, A.J.A., Sym, G., Avdic, K., Crawford, C., Duncan, A., Merrilees, D.W., 2008. Faecal indicator pollution from a dairy farm in Ayrshire, Scotland: source apportionment, risk assessment and potential of mitigation measures. Water. Res. 42 (4–5), 997–1012. https://doi.org/10.1016/j.watres.2007.09.015.

Woodward, S.J.R., Wöhling, T., Rode, M., Stenger, R., 2017. Predicting nitrate discharge dynamics in mesoscale catchments using the lumped StreamGEM model and bayesian parameter inference. J Hydrol. 552, 684–703. https://doi.org/10.1016/j.jhydrol.2017.07.021.

Yao, L., Zhang, J., Cao, C., Zheng, F., 2025. Parameter estimation and uncertainty quantification of rainfall-runoff models using data assimilation methods based on deep learning and local ensemble updates. Environ. Model. Softw. 185. https://doi.org/10.1016/j.envsoft.2025.106332.

Yuan, L., Sinshaw, T., Forshay, K.J., 2020. Review of watershed-scale water quality and nonpoint source pollution models. Geoscience 10 (1). https://doi.org/10.3390/geosciences10010025. MDPI AG.

Zimmer-Faust, A.G., Brown, C.A., Shanks, O.C., Rugh, W., Collura, T.C.M., Stecher, H.A., 2025. An integrated approach to coupled nutrient and microbial source tracking in an agricultural watershed. Water. Res. 272. https://doi.org/10.1016/j.watres.2024.122981.